Synthesis and Characterization of Epoxy Thermosetting Polymers from Glycidylated Organosolv Lignin and Bisphenol A

Lena Charlotte Over, Etienne Grau, Stéphane Grelier, Michael A. R. Meier, Henri Cramail

To cite this version:

HAL Id: hal-01611278

https://hal.science/hal-01611278

Submitted on 17 Nov 2019

Full Paper

Synthesis and characterization of epoxy <mark>resins</mark> from glycidylated organosolv lignin and bisphenol A[a]

Lena Charlotte Over, Etienne Grau, Stéphane Grelier, Michael A. R. Meier,* Henri Cramail*

_____

L. C. Over, Prof. M. A. R. Meier

Karlsruhe Institute of Technology (KIT), Institute of Organic Chemistry (IOC), Laboratory of Applied Chemistry, Straße am Forum 7, Building 30.48, D-76131 Karlsruhe, Germany. E-mail: m.a.r.meier@kit.edu

L. C. Over, Dr. E. Grau, Prof. S. Grelier, Prof. H. Cramail

Univ. Bordeaux, Laboratoire de Chimie des Polymères Organiques, UMR 5629, F-33607 Pessac Cedex, France. E-mail: cramail@enscbp.fr

Centre National de la Recherche Scientifique, Laboratoire de Chimie des Polymères Organiques, UMR 5629, F-33607 Pessac Cedex, France

_____

Abstract. Diglycidylether of bisphenol A (BPA) and isophorone diamine (IPDA) are industrially used for epoxy <mark>resin</mark> synthesis. Herein, glycidylated Organosolv lignin (GOL) is cured with DGEBA and IPDA for intensive studies. Organosolv lignin (OL) is therefore first glycidylated with epichlorohydrin to a material with an epoxy content of 3.2 mmol/g and analyzed *via* FTIR, ^{1}H and ^{31}P NMR. Epoxy resins with up to 42 wt% GOL are cured in DSC crucibles, analyzing the residual reaction heat. Characterization of dog bone shaped specimens is described with regard to structural properties from scanning electron microscopy (SEM) and FT-IR, thermal properties by differential scanning calorimetry (DSC) and thermogravimetric analysis (TGA), as well as mechanical properties by dynamic mechanical analysis (DMA) and stress/strain measurements. A lignin content between 8 and 33% leads to higher cross-linking density, resulting in a higher glass transition, lower swelling percentage and increased stiffness (Young's modulus) if compared to non-GOL resins.
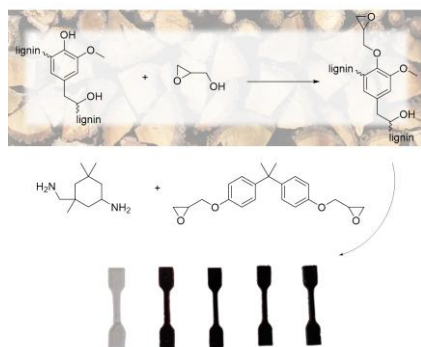
1 Introduction

Bisphenol-A (BPA) is one of the most produced chemicals worldwide and broadly used as monomer for polycarbonates, epoxy resins, polyesters or other polymers.[1] It finds applications in consumer products including food containers, bottles, tableware and paper for food packaging and medical equipment.[2] However, BPA exposure to the environment and to humans is followed by health concerns.[2–5] Although its activity as xenoestrogen is already known for decades,[6] the production volume in 2012 was 4.6 million tons, with a rising trend.[7] In addition to health care issues, BPA is obtained from fossil resources. The decreasing fossil feedstock is a growing problem demanding new synthetic routes from renewable resources. As one of the most abundant biopolymers on earth, lignin is a highly available renewable resource.[8] Due to its high aromatic content, it is investigated either for the replacement of aromatic monomers, obtained from lignin degradation (*e.g.*, vanillin, eugenol, other 4-substituted or 2-methoxy phenols[9–11]), or used as macromolecular structure for polymeric materials (*i.e.* in blends or composites). The monomer approach towards renewable based epoxy resins from lignin-obtained phenols was already intensively investigated. Vanillin-based epoxy resins were described in detail by Caillol *et al.*[12–14] Recently, epoxy thermosets from glycidylated *iso*-eugenol were presented.[15] In contrast, the macromolecular approach, *i.e.* the use of modified lignin as reactive monomer in epoxy resins, is more challenging due to the heterogenic structure of lignin and structural differences emerging through pulping procedures (Kraft, Organosolv, sulfite, pyrolysis, steam explosion,…).

The direct use of lignin as macromolecular structure in epoxy resins was limited for a long time to the use in blends and as ring-opening reagents.[16–22] In some cases, modification of lignin becomes necessary. For instance, hydroxy groups in lignin were converted to acidic

groups *via* esterification with succinic anhydride, increasing the reactivity towards epoxides.[23] In the last years, the interest for using lignin as epoxide compound increased and various approaches of using glycidylated lignin in epoxy resins were presented. Malutan *et al.* showed that the glycidylation of Kraft lignin depends on the origin of lignin and on different temperatures and reaction times.[24] For instance, wheat straw lignin lead to higher epoxy values than grass straw lignin under the same reaction conditions. Synthesis of cured epoxy resins with lignin are described with a) a conventional coating primer,[25] b) the diglycidylether of BPA (DGEBA) as additional epoxide compound and different hardeners (triethylenetatraamine,[26] 4,4'-diaminodiphenylmethane (DDM)[27,28] or a imidazole-based hardener[29]) or c) without a second epoxide compound, using a tung oil derived hardener[30] or a conventional novolac.[31] The various publications address different aspects of the characteristics of lignin-based resins. Some focus on thermal properties[27,31] and others analyze specific applications, such as epoxy asphalts[30] or coatings.[25] Recent publications examined the DSC curing behavior of lignin-based epoxy resins, analyzing the activation energy.[28,30]

In this work, the influence of macromolecular GOL content in a conventional epoxy resin with DGEBA was examined in detail. Isophorone diamine (IPDA) was chosen as cross-linker, since it is a common industrial amine hardener. A full analysis of basic properties is covered by analysis of curing behavior *via* DSC, structural information from IR and SEM, thermal properties from DSC and TGA, mechanical properties obtained by strain/stress measurement and DMA, as well as swelling in THF.

2   Experimental Section

2.1   Materials

The following chemicals were obtained from commercial sources and used without further purification:

Biphenol-A diglycidyl ether (sigma-aldrich), dichloromethane (sigma-aldrich), diphosphorous pentoxide (VWR), epichlorohydrin (sigma-aldrich), hydrochloric acid (37%, fisher scientific) isophorone diamine (TCI), magnesium sulfate (VWR), n-hexane (sigma-aldrich), sodium chloride (fisher scientific), potassium hydroxide (sigma-aldrich), pyridine (acros), tetrabutyl ammonium bromide (Acros), tetrahydrofuran (sigma-aldrich).

2.2 Reaction procedures

2.2.1 Organosolv Pulping

The Organosolv pulping was performed at the *Thünen Institute of Wood Research* (Hamburg, Germany). European beech wood (*F. sylvatica L.*) chips (10.8 kg) were treated with ethanol/water (50 v%) at 170 °C for 90 min with a catalytic amount H_2SO_4 (0.5 wt% based on dry wood). The solid to liquid ratio was 1:4. The lignin fraction in solution was separated from the solid fraction by filtration. Organosolv lignin (OL) was precipitated in water at a pH value of around 2. The suspension was centrifuged and OL separated. OL was dried at 40 °C in a vacuum drying oven and isolated as a brown solid (785 g, 7.8 wt%). The total hydroxy content of this unmodified lignin was calculated to be 4.53 mmol/g (from ^{31}P NMR analysis).

2.2.2 Glycidylation procedure

Organosolv lignin (25.0 g, 152 mmol OH) was suspended in epichlorohydrin (100 mL, 1.28 mol). Under ice cooling, tetrabutylammonium bromide, TBABr, (9.5 g, 29.6 mmol) was slowly added and the mixture stirred for 30 min. Portion-wise, potassium hydroxide (29.9 g, 534 mmol) was added over 2.5 hours. After stirring for another 5 hours at room temperature, the mixture was diluted with dichloromethane (300 mL) and extracted with water (3 × 200 mL). The aqueous phase was extracted with dichloromethane (2 × 50 mL) and the combined organic layers were washed with saturated sodium chloride solution (100 mL). After separation, the organic layer was dried over magnesium sulfate, filtrated and concentrated in a

rotary evaporator to 200 mL. The product was precipitated in n-hexane, filtrated and dried at 10^{-3} mbar over diphosphorous pentoxide.

^{1}H NMR (300 MHz, DMSO-d_6, δ): 6.87 – 6.61 (m, Ar H), 4.09 – 3.35 (m, -OCH$_3$, epoxy-CH), 2.86 – 2.55 (m, aliphatic H); IR (ATR): v = 3450 (br), 2994 (w), 2943 (w), 2873 (w), 1725 (w), 1597 (m), 1502 (m), 1457 (m), 1413 (m), 1330 (m), 1228 (m), 1125 (s), 1030 (m), 909 (m), 845 (m), 758 (w) cm^{-1}.

2.2.3 Preparation of epoxy resin

Glycidylated lignin and bisphenol-A diglycidyl ether were mixed in different ratios to a total amount of 1.50 g. Isophorone diamine was added in the ratio $n_{epoxide} : n_{amine} = 2 : 1$, giving a molar ratio of 1, as one amine can react with two epoxides. The materials were mixed homogeneously, poured into dog bone shaped molds and cured in the oven for 1 hour at 70 °C, then heated to 120 °C for 2 more hours.

2.3 Analytical procedures

2.3.1 Epoxy content titration

An exact amount (m_S) of approximately 200 mg glycidylated lignin was solved in 25.0 mL pyridine/HCl solution (Stock solution: 500 mL pyridine and 8.30 mL concentrated hydrochloric acid (37%)) and refluxed for 20 min at 115 °C. The sample solution was titrated with 2 M NaOH solution to neutral pH with a required volume V_s. A blank was measured using unmodified OL resulting in a required volume V_{blank}. The epoxy content (n_{epoxy}/g) was calculated as followed:

$$n_{epoxy}/g = \frac{(V_{blank} - V_S) * 2 \ mol/L}{m_S} \tag{1}$$

2.3.2 ^{1}H NMR Spectroscopy

^{1}H NMR spectra were measured in DMSO-d_6 with a Bruker AC 300 using 256 scans and a time delay $d1$ of 10 seconds at 25 °C. The sample concentration was 20 mg/mL. All ^{1}H NMR data are reported in ppm relative to the solvent signal for DMSO-d_6 at 2.50 ppm.

2.3.3 ^{31}P NMR Spectroscopy

An exact amount of 28–32 mg of the lignin sample was diluted in 400 µL CDCl$_3$/pyridine (1 : 1.6). 150 µL of a solution of chromium(III) acetylacetonate (3.6 mg/mL) as relaxation agent and cyclohexanol (4.0 mg/mL) as internal standard in CDCl$_3$/pyridine (1 : 1.6) were added and the solution was stirred for 5 minutes. 2-Chloro-4,4,5,5-tetramethyl-1,2,3-dioxapholane (70 µL) was added and the solution was transferred into a NMR tube for subsequent measurement in a Bruker Ascend^{TM} 400 MHz spectrometer with 512 scans, a delay time d1 of 5 seconds and a spectral width of 75 ppm (102 − 177 ppm). The chemical shifts are reported relative to the reaction product of 2-chloro-4,4,5,5-tetramethyl-1,2,3-dioxapholane with water at 132.2 ppm. Integrals are assigned to the functional groups as followed: δ = 150.0 − 145.5 (aliphatic hydroxy groups), 145.5 − 144.7 (cyclohexanol), 144.7 − 136.6 (phenolic hydroxy groups), 136.6 − 133.6 (carboxylic acids) ppm.[32] In the region of the phenolic hydroxy groups, syringyl (144.7 − 141.0 ppm) and guiacyl units (141.0 − 136.6 ppm) can be distinguished

2.3.4 Differential Scanning Calorimetry (DSC)

Differential Scanning Calorimetry (DSC) was performed on a DSC Q100 system from TA instruments. For reaction heat studies, 6 − 8 mg of the reaction mixture was heated in aluminum crucibles from 0 °C to 250 °C with a heating rate of 10 K min^{-1}.

The cured resin were analyzed with the following heating program with two cycles: first heating cycle: -50 °C − 200 °C (10 K min^{-1}); Cooling: 200 − -50 °C (-20 K min^{-1}), second heating cycle: -50 °C − 250 °C (10 K min^{-1}). The glass transition temperature (T_g) was defined

as the midpoint of the change in heat capacity occurring over the transition in the second heating cycle.

2.3.5 FT-IR Spectroscopy

Infrared spectra were recorded on a Bruker alpha-p instrument applying ATR technology.

2.3.6 Scanning electron microscopy (SEM)

SEM was performed on a HITACHI-S570 with an accelerating voltage of 12 kV. The surface was coated with gold by sputtering for 14 s prior to the measurements using a Balzers UNION SCD 040. Digital Image Scanning System and Processing System (DISS and DIPS) from point electronic were used to generate the images.

2.3.7 Thermogravimetric analysis (TGA)

Thermogravimetric analyses (TGA) were performed on a TGA-Q500 system from TA instruments at a heating rate of 5 K min^{-1} under synthetic air flow employing a sample mass of approximately 15 mg. From the two degradation temperatures of 5% ($T_{d\ 5\%}$) and 30% ($T_{d\ 30\%}$) weight loss, the statistic heat-resistant index (T_s) is calculated as follows:[33]

$$T_s = 0.49 \cdot \left(T_{d\ 5\%} + 0.6 \cdot (T_{d\ 30\%} - T_{d\ 5\%}) \right) \tag{2}$$

2.3.8 Dynamic Mechanical Analysis (DMA)

A DMA RSA 3 system from TA instruments was used to modulate from 25 °C to 240 °C at a heating rate of 5 K min^{-1}. The measurements were performed in 3-point bending mode at a frequency of 1 Hz, an initial force of 0.5 N and a strain sweep of 0.01%. The storage modulus E' is defined as the constant value below and over the glass transition. The glass transition temperature (T_g) is defined as the onset of the change in the storage modulus. The cross-linking density can be calculated from the following equation according to rubber elastic theory:[34]

$$\upsilon = \frac{E'}{\phi \cdot R \cdot (T_\alpha + 30\ K)} \tag{3}$$

where E' is the storage modulus of the cured resin in the rubbery state, ϕ is the front factor (approximately 1 in Flory theory[35]), R = 8.314 J mol^{-1} K^{-1} the gas constant and T_α is the maximum of tan delta (tan delta = E''/E', with E'' defined as loss modulus).

2.3.9 Stress/strain measurement

Stress/strain measurements were performed on a MTS Elite 25 system using a elongation at break method with dog bone shaped specimens (width = 2 mm; thickness = 2 mm and length of fixed section = 17.5 mm) using a 500 N load cell and a crosshead speed of 1 mm min^{-1}. Young's modulus (E) was determined from the linear part of the stress/strain curves for all samples.

2.3.10 Swelling properties

Swelling properties of weighted bar samples (m_0) of the cured resins were analyzed. After immersion in THF for 24 hours, the swollen samples were dried between paper and weighted again (m_{SW}). The samples were dried at 60 °C for 24 hours and weighted (m_D) to obtain the swelling percentage

$$Swelling\ (\%) = \frac{m_{SW} - m_D}{m_D} * 10 \tag{4}$$

and the soluble part of the networks

$$Soluble\ part\ (\%) = \left(1 - \frac{m_D}{m_0}\right) * 100 \tag{5}$$

3   Results and Discussion

3.1   Characterization of the glycidylated Organosolv lignin

OL was isolated at Thünen Institute of Wood Research *via* an ethanol—water pulping and used without further fractioning (for details, see experimental part). A full characterization of this batch OL can be found in the literature.[36] Glycidylation of OL with epichlorohydrin in the presence of NaOH and TBABr was performed without external heating. The exothermic

reaction led to heat evolution, so that ice cooling was necessary in the first hours to avoid temperatures above 50 °C. In literature, the increase of reaction temperatures from 50 to 70 or 90 °C led to lower epoxy contents.[24,37] However, no reaction conditions at room temperature are described. In the present work, a lignin epoxy material with an epoxy content of 3.2 mmol/g was obtained. The value is in the range of similarly functionalized steam exploded lignin[29,31] or Organosolv lignin[27] and higher than for glycidylated Kraft or acetic acid lignin.[24,26,37] The comparison reveals that Organosolv and steam exploded lignin result in higher epoxy contents. A reason for this behavior may be the better solubility and lower molar mass of these lignins. Moreover, a higher aromatic hydroxyl group content in these lignins is present due to the pulping conditions. In addition to the titration result, ^{31}P NMR was performed. The glycidylated compound showed a decrease of the aromatic hydroxy groups from 1.83 mmol/g to 0 mmol/g, indicating that all phenolic groups reacted (Table 1). The value for the aliphatic hydroxy groups decreased from 2.70 to 1.92 mmol/g leading to an overall functionalization of at least 2.6 mmol/g. The value is lower than the one obtained from titration, which may indicate that epoxy rings were partially opened. A ring opening with water as nucleophile would result in two new aliphatic hydroxy groups, explaining a small increase of aliphatic hydroxy groups and the change in signal shape of the aliphatic region (for ^{31}P spectra, see SI).

Table 1. Characteristics of unmodified and glycidylated lignin.

Quantity	Epoxy content[a] [mmol/g]	Aliphatic OH content[b] [mmol/g]	Aromatic OH content[b] [mmol/g]	Total OH content[b] [mmol/g]
unmodified OL	0	2.70	1.83	4.53
glycidylated OL	3.2	1.92	0	1.92

[a]from titration; [b] from ^{31}P analysis

FT-IR analysis of glycidylated lignin revealed a significant decrease of hydroxy group stretching vibrations at ~3450 cm^{-1} (Figure 1), indicating their functionalization. In addition, a new signal appeared at 909 cm^{-1}, which is typical for the asymmetric stretching vibration band of C-O-C in epoxy functions.[38] Vibrations of ether linkages, such as the newly formed C-O-glycidyl, show typical bands in the region between 1000 and 1200 cm^{-1}. Here, a significant increase was observed. The signals of the functional groups that did not take place in the modification procedure, such as C-H bonds (2600 – 3000 cm^{-1}) and aromatic C=C bonds (1502 and 1597 cm^{-1}), did not change. The results are in agreement with previous reported FT-IR spectra for glycidylated lignins.[24,26,29–31,37]
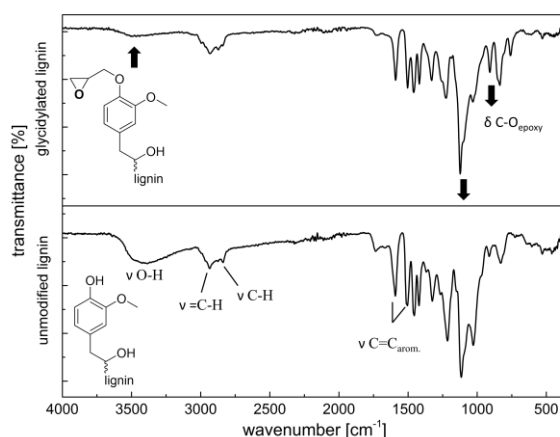
Figure 1. FT-IR spectra (ATR) of modified, glycidylated lignin (top) and unmodified lignin (bottom).

Analyzing the degradation temperature for 5% weight loss ($T_{d\ 5\%}$), the thermal stability revealed an increase accompanied with glycidylation, from 233 to 269 °C (for TGA traces, see SI). The main difference occurred during the first 30% weight loss. At the $T_{d\ 30\%}$ value, the degradation traces assimilated. Both traces showed two main degradation steps. This first degradation process between 280 and 350 °C can be assigned to inter-unit ether bond cleavage in lignin. This results in evaporation of volatile aromatic compounds.[39,40] A second step occurs between 500 and 600 °C. At this temperature, aromatic rings are expected to decompose.[41] This two-step degradation is characteristic for cross-linked materials with

aromatic and ether functional groups as in lignin. This first degradation step is more relevant for glycidylated lignin compared to unmodified lignin as there are additional ether functions in the product. Increased degradation temperatures for glycidylated lignin compared to unmodified lignin are described in literature for Kraft lignin[37] as well as for Organosolv lignin.[42]

3.2 Curing behavior of lignin reinforced epoxy resin

The curing behavior of lignin reinforced epoxy resins was investigated *via* DSC studies. GOL and DGEBA were mixed with different lignin contents (0 to 50 wt% of the epoxy part, which is 0 to 42 wt% of the resin) and with a stoichiometric amount of IPDA. IPDA contains two amines – an aliphatic amine and a cycloaliphatic amine. Each amine can react with two epoxides.[43] Thus, the molar ratio r is calculated as followed:

$$r = \frac{f_{DGEBA} \cdot n_{epoxy}(DGEBA) + n_{epoxy}(GOL)}{f_{amine} \cdot n_{amine}} \tag{6}$$

assuming that the functionality of IPDA (f_{amine}) is equal to 4 and the functionality of DGEBA (f_{DGEBA}) is equal to 2 and the molar quantities of amine, DGEBA and GOL are assigned to n_{amine}, $n_{epoxy}(DGEBA)$ and $n_{epoxy}(GOL)$, respectively. Hence, a stoichiometric amount is defined by a ratio r = 1 and usually leads to the highest thermomechanical properties.[44]

The recorded DSC traces for different lignin contents in the final resin are shown in **Figure 2a.** The heating revealed an exothermic peak with a starting point at 50 °C, a maximum around 110 °C and end point at 220 °C. The maximum shifts slightly to lower temperature, from 114 °C to 100 °C, with increased lignin content of 0 wt% to 42 wt%, respectively. A shoulder, observed at 150 °C, decreases in intensity with increasing lignin content. The two peaks result from the difference in reactivity of the aliphatic and cyclo-aliphatic amino groups in IPDA. Cyclo-aliphatic amines are less reactive than aliphatic amines.[43] A reason for the decrease of the shoulder and the shift of the maximum with increased lignin content may be assigned to the remaining free hydroxy groups in lignin, that react with epoxides, hindering

amines to react. Usually, the reaction of hydroxy groups with epoxides is only relevant if excess of epoxides are used.[43] Yet, the sterically hindered structure of lignin may favor this reaction.

The residual reaction heat ΔH of the curing process is plotted against the lignin content in the final resin (**Figure 2b**). ΔH in J/g decreases with increasing lignin content from 385 J/g for 0 wt% to 291 J/g for 42 wt% (Figure 2b, black). The ΔH value for the lignin-free DGEBA-IPDA resin is in the order of literature values.[44][45] To the best of our knowledge, no residual heat reaction was analyzed for lignin-based epoxy resins in literature before. Simultaneously with the reaction heat decrease, the epoxy group content in the uncured mixture decreases from 5.88 to 4.54 mmol/g. Considering this decrease, the reaction heat varies between 56 and 66 J/mmol epoxide without significant increase or decrease tendency (Figure 2**b**, grey), indicating that the reactivity of the epoxides in glycidylated lignin and DGEBA is similar.
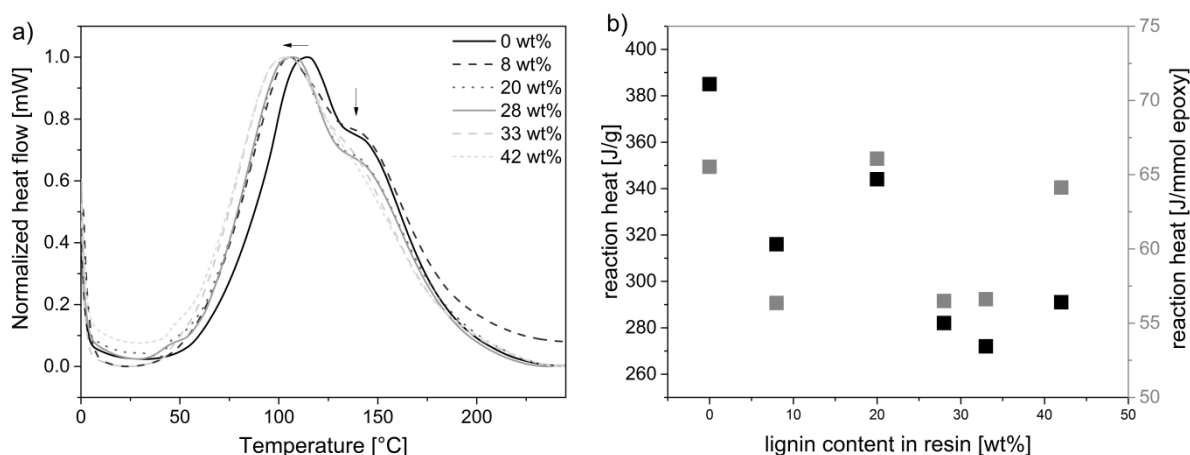
Figure 2. a) Normalized DSC traces of the curing of DGEBA-based epoxy resins (lignin content in wt%) at a heating rate of 10 K min^{-1}; b) Reaction heat in J/g (left axis, black) and in J/mmol epoxy (right axis, grey).

3.3 Structure of cured resins

The final resins were cured in an oven at 70 °C for 1 hour and 120 °C for 2 hours in dog bone shape silicon molds to obtain specimens for direct structural and thermomechanical analyses.

Comparison of the IR region between 500 and 1800 cm^{-1} for cured epoxy resins with uncured GOL shows the decrease of the epoxy C-O deformation vibration band for resins with lignin contents between 0 and 33 wt.% (**Figure 3**). Only for the resin with 42 wt.% GOL, the signal at 909 cm^{-1} is still present, indicating an inefficient curing process. Other changes in signal in Figure 3 can be explained as followed from the lowest wavenumber going to the highest. The broad signal at < 600 cm^{-1} results from skeletal C-C-C and H-C-C deformation vibrations mainly found in BPA and IPDA. The increased signal at 830 cm^{-1} should mainly result from the C-H deformation vibration in the 1-4 substituted BPA.[46] C-N stretching vibrations of tertiary amines contained in the cured resins show a typically bands at 1070 cm^{-1}. The signal is overlaying with the symmetric C-O-C stretching vibration of aromatic ether and the C-H deformation vibration of 1-4 substituted BPA. Likewise, the new signal at 1180 cm^{-1} can be assigned to the deformation vibration of benzylic C-H in BPA. Aromatic ether in BPA shows a broad band for the asymmetric C-O-C stretching vibration at 1233 cm^{-1}. Due to the different origin of the C=C stretching vibrations in the aromatic rings of BPA compared to GOL, two signals can be found, at 1581 and 1608 cm^{-1}. All in all, the IR analysis showed the expected changes and proved the reaction of the epoxides. Only in the case of the highest applied lignin content, no efficient reaction was observed. The reason for inefficient reaction may be the poor miscibility of glycidylated lignin, DGEBA and IPDA due to the high solid-to-liquid ratio. Because of miscibility issues, no higher lignin contents were evaluated.
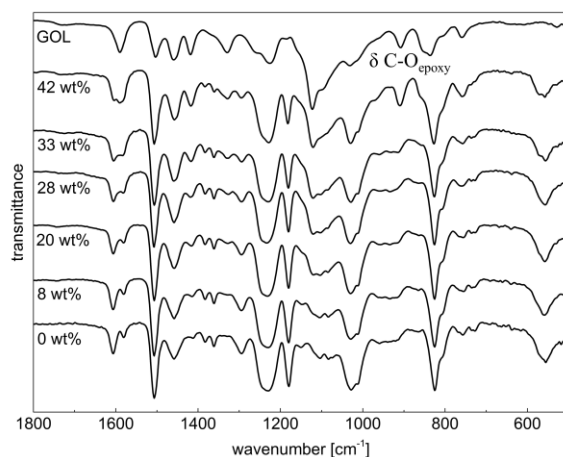
Figure 3. IR spectra (ATR) of glycidylated OL and cured epoxy resins.

SEM images with a magnitude of 5000 of the different resins are shown in **Figure 4a-f**. Cured resins were analyzed at a breaking edge. In all resins, the break caused the visible lamellar structure. Within the structure, homogeneity differences can be observed. The addition of lignin caused the formation of small dots, increasing in number with increasing GOL content. These dots are not observed in lignin-free epoxy resin (Figure 4**a**). With 8, 20 and 28 wt.% GOL in the resin, the structure is mostly homogeneous (Figure 4**b-d**). In the resins with the highest lignin amounts of 33 and 42 wt.% (Figure 4**e and f**), the agglomerations increased compared to lower lignin contents, indicating the partial incompatibility with the epoxy resin. This incompatibility can be explained by the inhomogeneous structure of lignin itself. Compared to literature results of SEM images for lignin-based epoxy resin, the herein discussed GOL still shows a better resin compatibility at higher lignin content: acetic acid lignin-based epoxy resin curing with DGEBA and triethylenetetramine led to higher agglomeration and even porosity if 50% of DGEBA were replaced.[26]

- 15 -
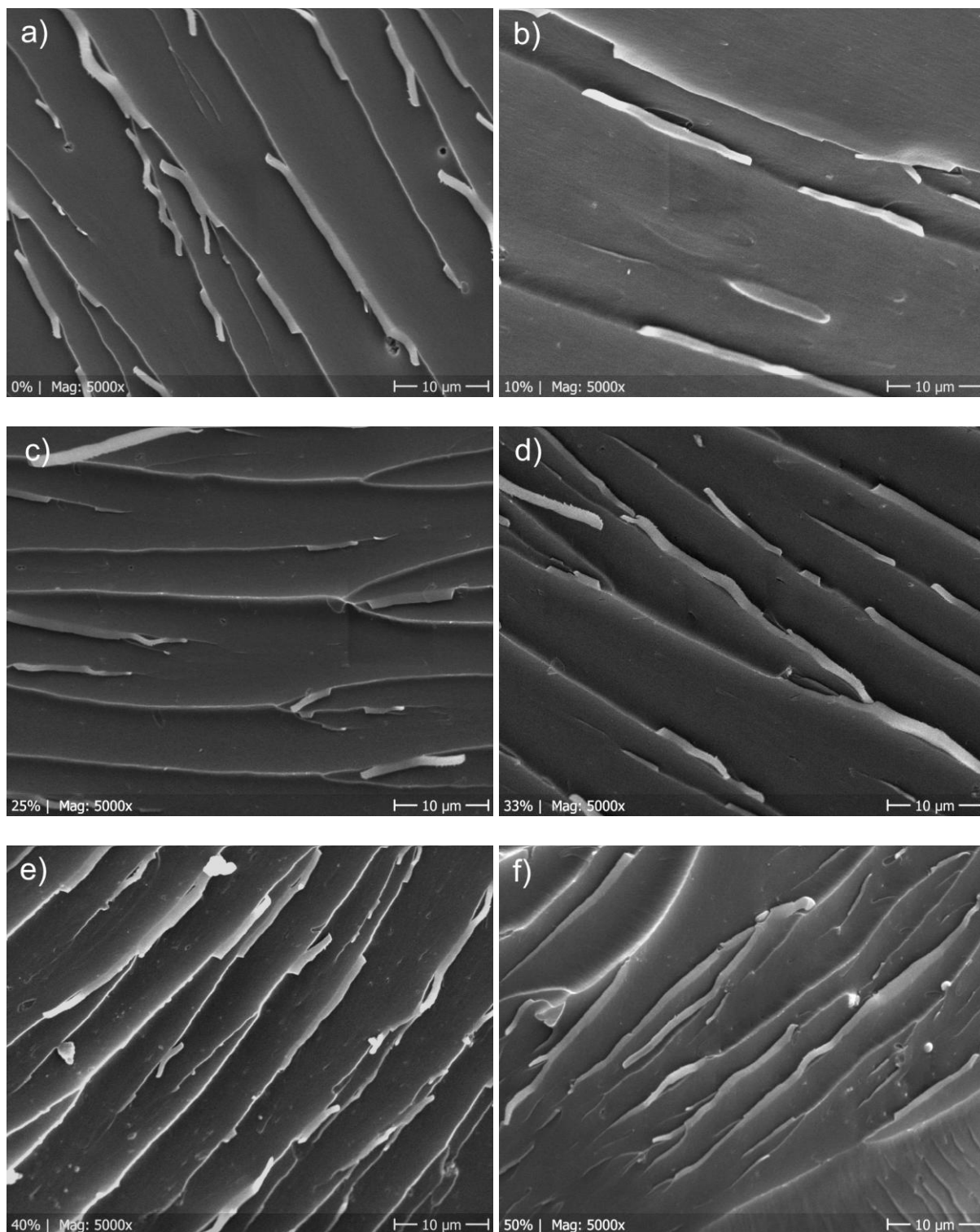
Figure 4. SEM images with 5000x magnification at the breaking edge of epoxy resins with a) 0 wt%, b) 8 wt%, c) 20 wt%, d) 28 wt%, e) 33 wt%, and f) 42 wt% GOL in the final resin (the shown percentages indicate the DGEBA replaced by GOL).

3.4 Thermomechanical properties of epoxy resins from DGEBA and glycidylated lignin

The influence of the lignin content on thermomechanical properties was studied by TGA, DSC, DMA and stress/strain measurements. The degradation temperature for 5% weight loss ($T_{d\,5\%}$), measured *via* TGA, decreases from 334 °C to 284 °C, with increasing lignin content (**Figure 5a**). Regarding the weight loss trace (**Figure 5b**), the degradation temperature for 30% weight loss ($T_{d\,30\%}$) is in a narrower region between 338 and 350 °C. Likewise, the lignin-free composite is the most stable resin. The heat resistant index T_s, calculated from Equation (2), varies between 168 and 156 °C and thus, also decreases with increasing lignin content. Although this initial degradation starts at higher temperatures for lignin-free resin, the second degradation step starts later for lignin-containing resins. Earlier initial degradation for lignin-containing resins coincides with observations for other lignin-DGEBA[26] and lignin epoxy resins without second epoxy compound.[29,31] The first degradation, as discussed for the unmodified and glycidylated lignin, occurs mainly between 280 and 350 °C and is most significant for all samples. A second degradation step from further cracking processes occurs between 500 and 600 °C. Since this behavior hardly changes with the addition of lignin, the similar characteristics of linkages in lignin-based and lignin-free epoxy material is exhibited.
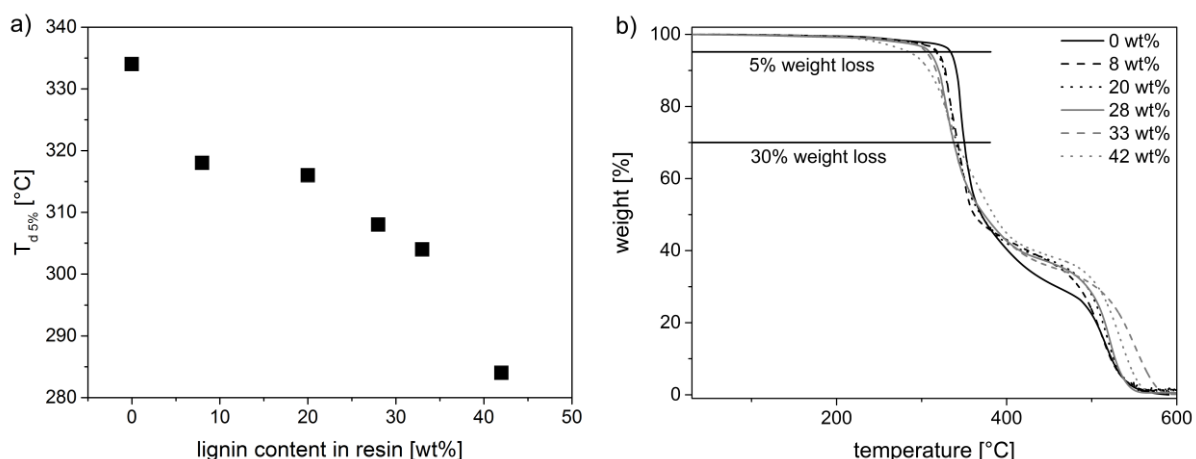
Figure 5. a) Degradation temperature for 5% mass loss for the cured resins with different lignin content obtained from TGA; b) Comparison of the weights loss during TGA for the different cured resins at a heating rate of 5 K min^{-1}.

The glass transition temperature (T_g) was evaluated from DSC and DMA measurements (**Figure 6**). T_g increases from 150 °C to 168 °C (DSC), with increasing lignin content from 0 to 33 wt%. DMA results show the same tendency, with T_g values ranging from 123 to 138 °C. Going to 42 wt% lignin, T_g drops to 132 °C (for DMA; no T_g observed in DSC). An increased T_g may indicate a higher cross-linking density in the resin.[43] Glycidylated lignin contains free hydroxy groups that could react with epoxies, leading to higher cross-linking. On the other hand, the inhomogeneous structure of lignin may lead to a more rigid structure, also leading to a higher T_g.
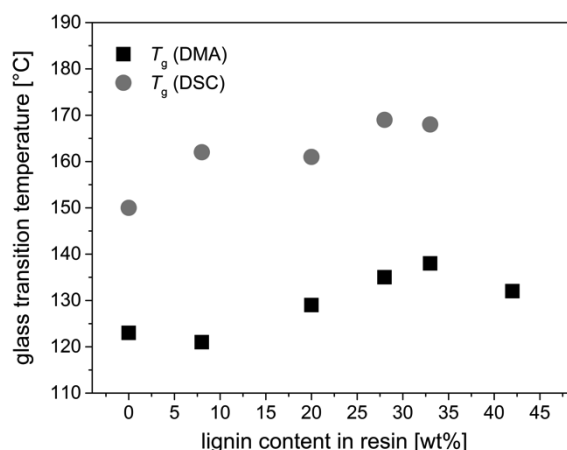
Figure 6. Glass transition temperature of the cured resins with different lignin content obtained from DSC (grey) and DMA (black).

Mechanical properties of the resins from stress/strain and DMA measurements are shown in **Table 2**. Young's modulus E varied between 1.82 and 1.88 GPa. This is within expectations for DGEBA-based epoxy resins. In literature, values around 3 GPa are reported.[47,48] 10% replacement of DGEBA by lignin led to a drop of E from 1.88 to 1.82 GPa. A low lignin amount seems to add flexibility to the resin, which may be explained by lower epoxy density. Going to a higher lignin content (50 wt% of DGEBA were replaced by GOL), the product became more rigid (E increases), leading to a brittle material that could not be fixed to the apparatus without breaking immediately. The increase of E, accompanied by higher stiffness, results from the inhomogeneous structure of lignin. This observation coincides with the increasing glass transition with increasing lignin content. The storage modulus E' in the glassy state obtained from DMA was in a similar region and showed the same tendency as E. Likewise, the observed decrease in the elongation at break for higher GOL content indicates a higher stiffness (Table 2, column 3). The cross-linking density, calculated from Equation (3) from the storage modulus E' in the rubbery phase and T_α, showed an increase with growing lignin content, as already estimated from the glass transition. BPA-IPDA resins exhibited a cross-linking density υ of $9.9 \cdot 10^3$ mol m^{-3} and the resins with 28 and 33 wt% lignin showed densities of 23 and $22 \cdot 10^3$ mol m^{-3}, respectively. Only for the resin with the highest lignin

content of 42 wt%, a decrease was observed. The already discussed for other analytics, the GOL is poorly miscible with DGEBA and IPDA if the lignin-content is to high und thus, no satisfying results can be obtained. The optimum can be found for a resin with 33 wt% of GOL.

Table 2. Values for mechanical properties and swelling test of cured lignin-BPA-IPDA-based epoxy resins

Lignin content [%]	Young's modulus [GPa]	Elongation at break [%]	E' (36 °C) [GPa]	E' (210 °C) [GPa]	T_α [°C]	υ [10^3 mol m^{-3}]
0	1.88	3.0	1.37	0.036	137	9.8
8	1.82	2.3	2.02	0.048	138	13
20	1.84	2.0	1.95	0.055	148	15
28	1.92	1.5	1.9	0.087	157	23
33	1.90	1.70	1.84	0.083	159	22
42	samples broke during traction test preparation		1.07	0.033	144	8.8

3.5 Swelling properties

The swelling of the cured resins was performed in THF as described in section 2.3.10 in the experimental part. Swelling and soluble part were calculated from Equation (4) and (5), respectively, and summarized for all lignin contents (**Table 3**). A lower percentage of swelling usually indicates a higher cross-linking density, as distances within the network are smaller and thus, solvent absorption is lower as well. Swelling decreased from 7 to 1%, in tandem with increased lignin content from 0 to 20 wt%. This implies a higher cross-linking with a lignin content of 20 wt%. Higher lignin contents resulted in increased swelling up to 10% for 42 wt% GOL. The soluble part remained constantly low and then increased with increased lignin content from 0% soluble part for 0, 8 or 20 wt% lignin content to 6% soluble part for 42 wt% lignin content. As estimated from T_g and calculated from DMA, the swelling

test revealed the same tendency. The addition of lignin initially stabilized the epoxy resin product due to a higher cross-linking, but led to poor network formation with lignin content of 42 wt%.

Table 3. Swelling properties of cured epoxy resins

Lignin content [%]	0	8	20	28	33	42
Swelling [%]	7	3	1	3	2	10
Soluble part [%]	0	0	0	1	1	6

4   Conclusion

Epoxy resins were synthesized from glycidylated organosolv lignin and DGEBA in different weight ratios and IPDA as common industrial hardener. Under the chosen conditions, lignin could not completely replace BPA. However, in the applied weight ratios, lignin revealed reinforcing properties with weight percentages up to 33% in the final product. DSC curing verified the replacement suitability, indicating a similar reactivity for lignin- and BPA-based epoxides. The completed reaction in the final resins was verified by the disappearance of the epoxy stretching vibration band in IR spectroscopy. In addition, thermal and mechanical analysis revealed that lignin-based resins have a higher cross-linking density compared to pure DGEBA-IPDA resin, if 10 to 40 wt.% of DGEBA was replaced. Although, thermal stability decreases with increasing lignin content, degradation temperatures are still in an applicable region for epoxy resins. Due to inhomogeneity in lignin itself, inhomogeneity in the produced resins was observed if the renewable content is increased but can still be considered low. All in all, it could be shown that GOL is suitable for partial replacement of DGEBA in an industrial relevant epoxy resin.

Supporting Information

Supporting Information is available from the Wiley Online Library or from the author.

Appendix

[1]   T. Geens, L. Goeyens, A. Covaci, *Int. J. Hyg. Environ. Health* **2011**, *214*, 339.

[2]   M. Bondesson, J. Jönsson, I. Pongratz, N. Olea, J.-P. Cravedi, D. Zalko, H. Håkansson, K. Halldin, D. Di Lorenzo, C. Behl, D. Manthey, P. Balaguer, B. Demeneix, J.-B. Fini, V. Laudet, J.-A. Gustafsson, *Reprod. Toxicol.* **2009**, *28*, 563.

[3]   H. H. Le, E. M. Carlson, J. P. Chua, S. M. Belcher, *Toxicol. Lett.* **2008**, *176*, 149.

[4]   L. N. Vandenberg, R. Hauser, M. Marcus, N. Olea, W. V. Welshons, *Reprod. Toxicol.* **2007**, *24*, 139.

[5]   J. H. Kang, F. Kondo, Y. Katayama, *Toxicology* **2006**, *226*, 79.

[6]   E. C. Dodds, W. Lawson, *Nature* **1936**, *137*, 996.

[7]   Merchant Research & Consulting: World BPA Production, https://mcgroup.co.uk/, accessed: July, 2016.

[8]   R. Whetten, R. Sederoff, *Plant Cell* **1995**, *7*, 1001.

[9]   J. Zakzeski, P. C. A. Bruijnincx, A. L. Jongerius, B. M. Weckhuysen, *Chem. Rev.* **2010**, *110*, 3552.

[10]   M. Kleinert, T. Barth, *Chem. Eng. Technol.* **2008**, *31*, 736.

[11]   M. P. Pandey, C. S. Kim, *Chem. Eng. Technol.* **2011**, *34*, 29.

[12]   M. Fache, A. Viola, R. Auvergne, B. Boutevin, S. Caillol, *Eur. Polym. J.* **2015**, *68*, 526.

[13]   M. Fache, R. Auvergne, B. Boutevin, S. Caillol, *Eur. Polym. J.* **2015**, *67*, 527.

[14]   M. Fache, B. Boutevin, S. Caillol, *Green Chem.* **2016**, *18*, 712.

[15]   C. François, S. Pourchet, G. Boni, S. Fontaine, Y. Gaillard, V. Placet, M. V. Galkin, A. Orebom, J. Samec, L. Plasseraud, *RSC Adv.* **2016**, *6*, 68732.

[16]   C. I. Simionescu, V. Rusan, M. M. Macoveanu, G. Cazacu, R. Lipsa, C. Vasile, A. Stoleriu, A. Ioanid, *Compos. Sci. Technol.* **1993**, *48*, 317.

[17]   D. Feldman, D. Banu, A. Natansohn, J. Wang, *J. Appl. Polym. Sci.* **1991**, *42*, 1537.

[18]   D. Feldman, D. Banu, C. Luchian, J. Wang, *J. Appl. Polym. Sci.* **1991**, *42*, 1307.

[19]   Y. Nonaka, B. Tomita, Y. Hatano, *Holzforschung* **1997**, *51*, 183.

[20]   D. Feldman, M. Khoury, *J. Adhes. Sci. Technol.* **1988**, *2*, 107.

[21]   Q. F. Yin, M. W. Di, *Adv. Compos. Mater. Pts 1-3* **2012**, *482-484*, 1959.

[22]   G.-H. Delmas, B. Benjelloun-Mlayah, Y. Le Bigot, M. Delmas, *J. Appl. Polym. Sci.* **2013**, *127*, 1863.

[23]   S. Hirose, T. Hatakeyama, H. Hatakeyama, *Macromol. Symp.* **2003**, *197*, 157.

[24]   T. Malutan, R. Nicu, V. I. Popa, *BioResources* **2008**, *3*, 1371.

[25]   A. Singh, K. Yadav, A. Kumar Sen, *Am. J. Polym. Sci.* **2012**, *2*, 14.

[26]   P. Feng, F. Chen, *BioResources* **2012**, *7*, 2860.

[27]   F. Ferdosian, Z. Yuan, M. Anderson, C. C. Xu, *J. Anal. Appl. Pyrolysis* **2016**, *119*, 124.

[28]   F. Ferdosian, Y. Zhang, Z. Yuan, M. Anderson, C. Xu, *Eur. Polym. J.* **2016**, *82*, 153.

[29]   C. Sasaki, M. Wanaka, H. Takagi, S. Tamura, C. Asada, Y. Nakamura, *Ind. Crops*

Prod. **2013**, *43*, 757.

[30] J. Xin, M. Li, R. Li, M. P. Wolcott, J. Zhang, *ACS Sustain. Chem. Eng.* **2016**, *4*, 2754.

[31] C. Asada, S. Basnet, M. Otsuka, C. Sasaki, Y. Nakamura, *Int. J. Biol. Macromol.* **2015**, *74*, 413.

[32] A. Granata, D. S. Argyropoulos, *J. Agric. Food Chem.* **1995**, *43*, 1538.

[33] Y. C. Chiu, I. C. Chou, W. C. Tseng, C. C. M. Ma, *Polym. Degrad. Stab.* **2008**, *93*, 668.

[34] T. Iijima, N. Yoshioka, M. Tomoi, *Eur. Polym. J.* **1992**, *28*, 573.

[35] P. J. Flory, *Polymer* **1979**, *20*, 1317.

[36] L. C. Over, M. A. R. Meier, *Green Chem.* **2016**, *18*, 197.

[37] N.-E. El Mansouri, Q. Yuan, F. Huang, *BioResources* **2011**, *6*, 2647.

[38] M. G. González, J. C. Cabanelas, J. Baselga, *Infrared Spectroscopy – Materials Science, Engineering and Technology*, INTECH **2012**, Ch. 13.

[39] H. El-Saied, A. A. M. A. Nada, *Polym. Degrad. Stab.* **1993**, *40*, 417.

[40] R. Sun, J. Tomkinson, G. Lloyd Jones, *Polym. Degrad. Stab.* **2000**, *68*, 111.

[41] H. Yoshida, R. Mörck, K. P. Kringstad, *Holzforschung* **1987**, *41*, 171.

[42] F. Ferdosian, Z. Yuan, M. Anderson, C. C. Xu, *J. Sci. Technol. For. Prod. Process.* **2012**, *2*, 11.

[43] R. Auvergne, S. Caillol, G. David, B. Boutevin, J. P. Pascault, *Chem. Rev.* **2014**, *114*, 1082.

[44] J. Galy, A. Sabra, J. Pascault, *Polym. Eng. Sci.* **1986**, *26*, 1514.

[45] M. Chrysanthos, J. Galy, J.-P. Pascault, *Polymer* **2011**, *52*, 3611.

[46] A. Cherdoud-Chihani, M. Mouzali, M. J. M. Abadie, *J. Appl. Polym. Sci.* **2003**, *87*, 2033.

[47] A. A. Roche, J. Bouchet, *Application of Fracture Mechanics to Polymers, Adhesives and Composites*, 1st ed., Elsevier Ltd and ESIS **2004**, pp. 249-257.

[48]   T. Okabe, Y. Oya, K. Tanabe, G. Kikugawa, K. Yoshioka, *Eur. Polym. J.* **2016**, *80*, 78.

Epoxy resins from glycidylated organosolv lignin, diglycidyl ether of bisphenol A (DGEBA) and isophorone diamine (IPDA) are discussed for lignin contents between 0 and 42 wt%. Lignin-based resins show higher cross-linking densities that lead to higher glass transition, lower swelling percentages and increased stiffness if compared to non-lignin resins.

L. C. Over, E. Grau, S. Grelier, M. A. R. Meier,* H. Cramail*

Synthesis and characterization of epoxy resins from glycidylated organosolv lignin and bisphenol A

Supporting Information

Synthesis and characterization of epoxy resins from glycidylated organosolv lignin and bisphenol A

Lena Charlotte Over, Etienne Grau, Stéphane Grelier, Henri Cramail, Michael A. R. Meier*

Characterization of glycidylated lignin

^{1}H NMR
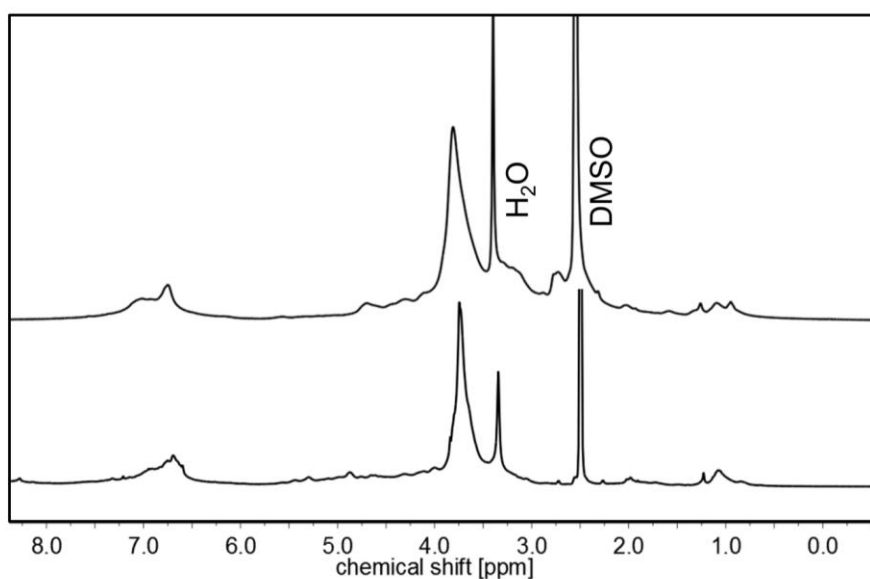
^{31}P NMR spectra
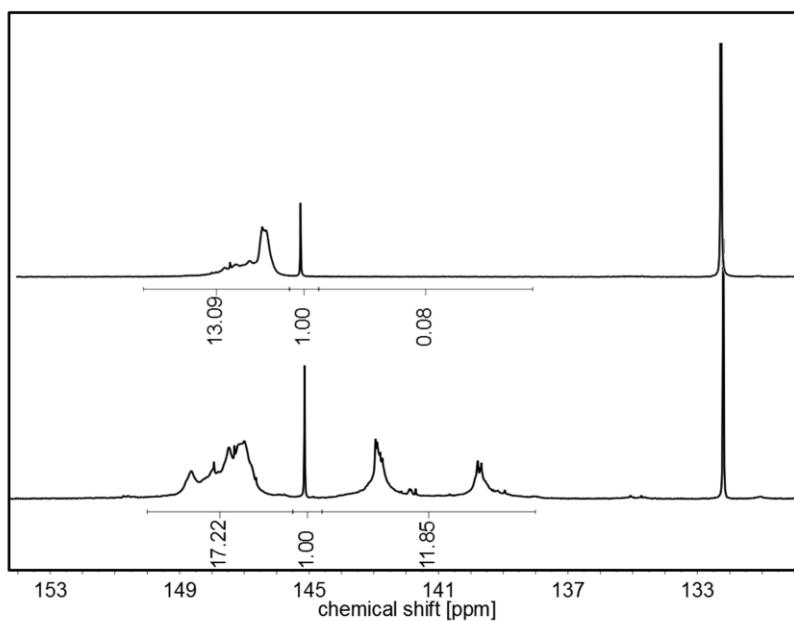
Figure 7. ^{31}P NMR spectra of unmodified organsolv lignin (top) and glycidylated lignin (bottom).

Thermogravimetric analysis (TGA)
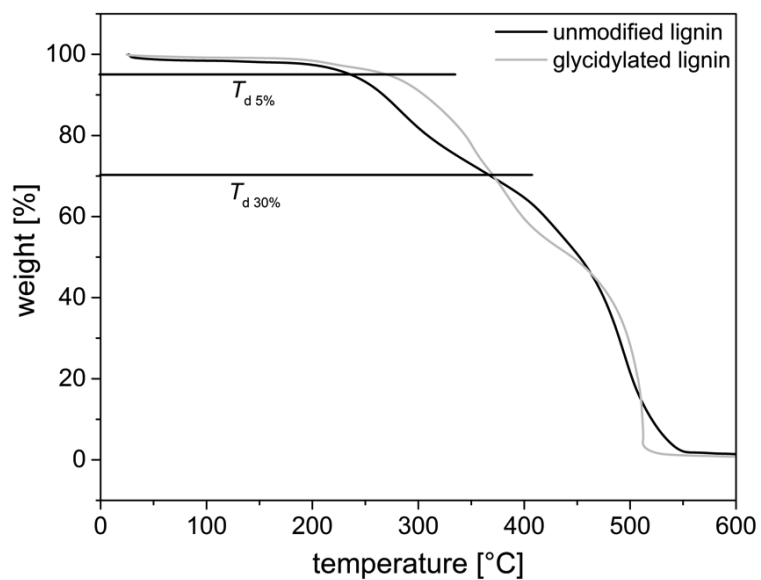
Figure 8. TGA traces of unmodified and glycidylated lignin.

Characterization of the resin

Thermogravimetric analysis

Table 4. Thermogravimetric analysis: degradation temperature for epoxy resins with different lignin contents.

Lignin content [%]	$T_{d\,5\%}$ [°C]	$T_{d\,30\%}$ [°C]	T_S [°C]
unmodified lignin	233	265	153
glycidylated lignin	269	371	162
0	334	350	168
8	318	343	163
20	316	341	162
28	308	338	160
33	304	338	159
42	284	342	156

Differential scanning calorimetry (DSC)
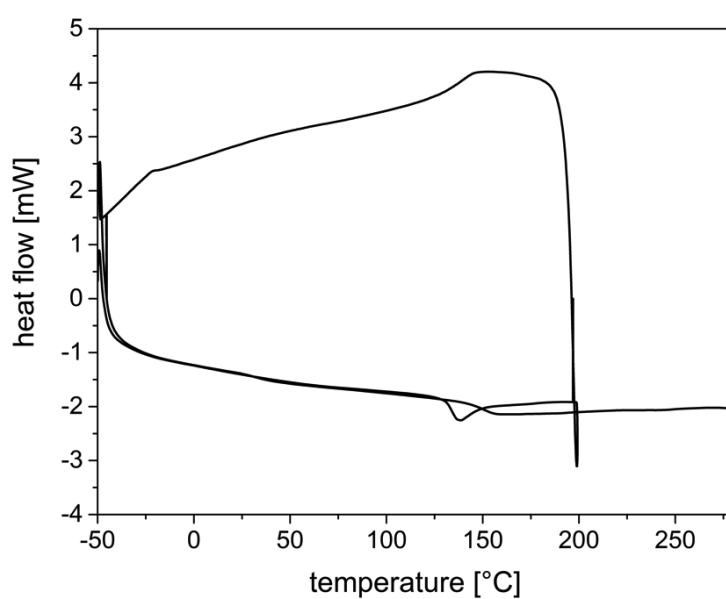
Figure 9. DSC trace for cured epoxy resin from DGEBA and IPDA (0 wt% lignin).
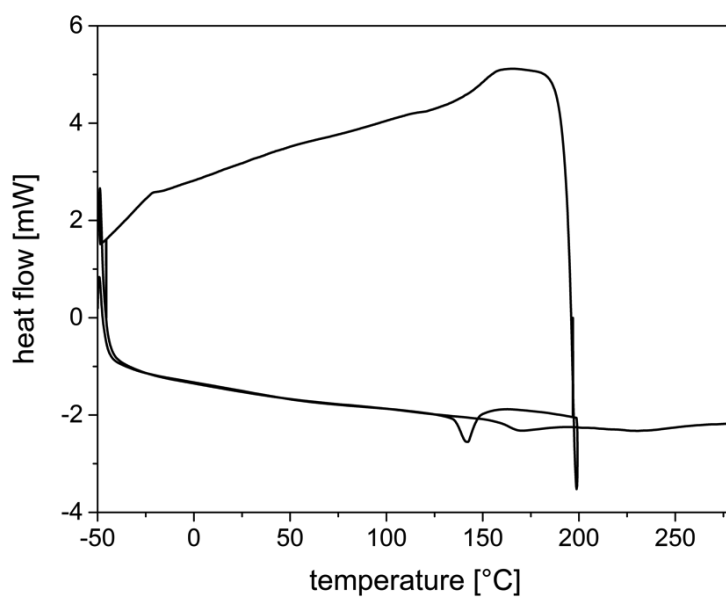
Figure 10. DSC trace for cured epoxy resin with 8 wt% glycidylated lignin.
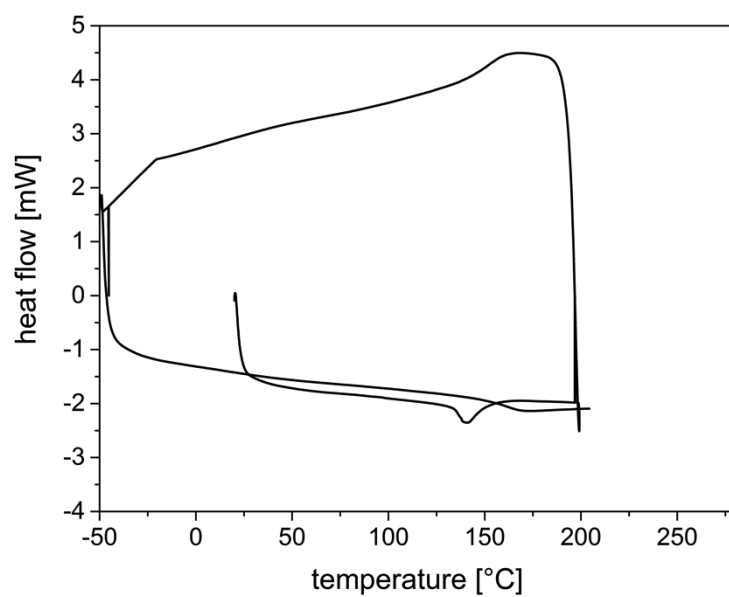
Figure 11. DSC trace for cured epoxy resin with 20 wt% glycidylated lignin.
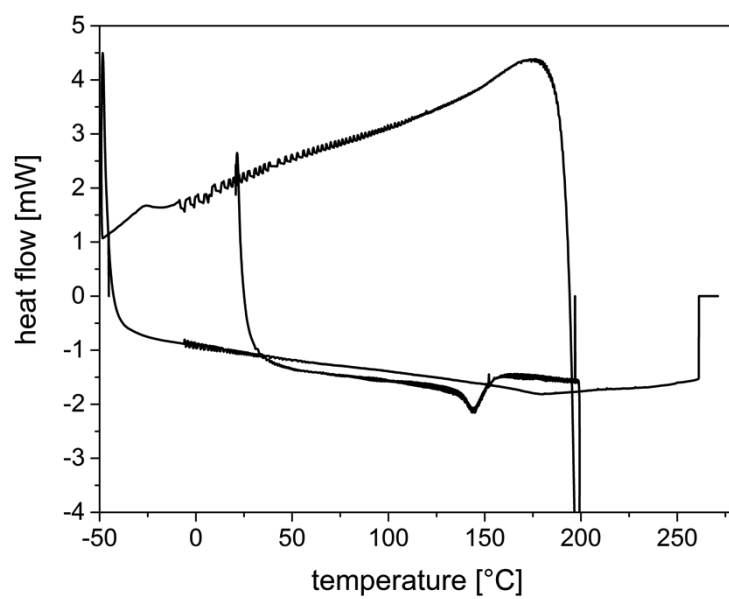
Figure 12. DSC trace for cured epoxy resin with 28 wt% glycidylated lignin.
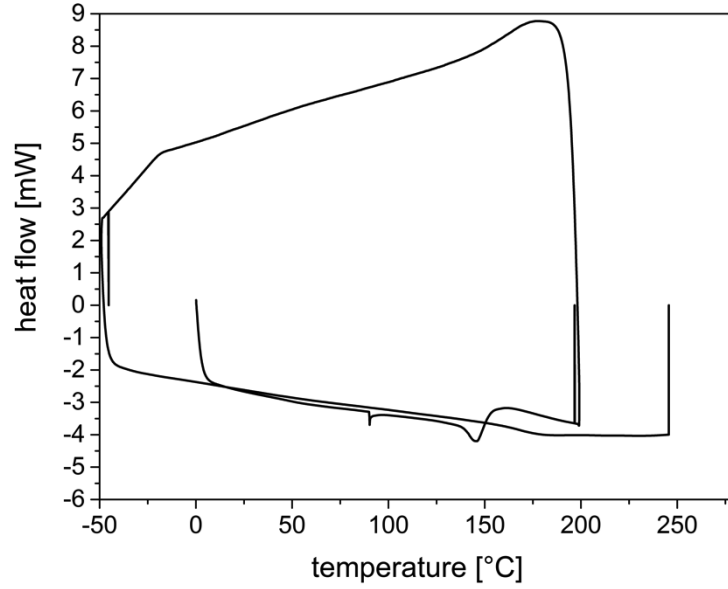
Figure 13. DSC trace for cured epoxy resin with 33 wt% glycidylated lignin.

Dynamic mechanical analysis (DMA)
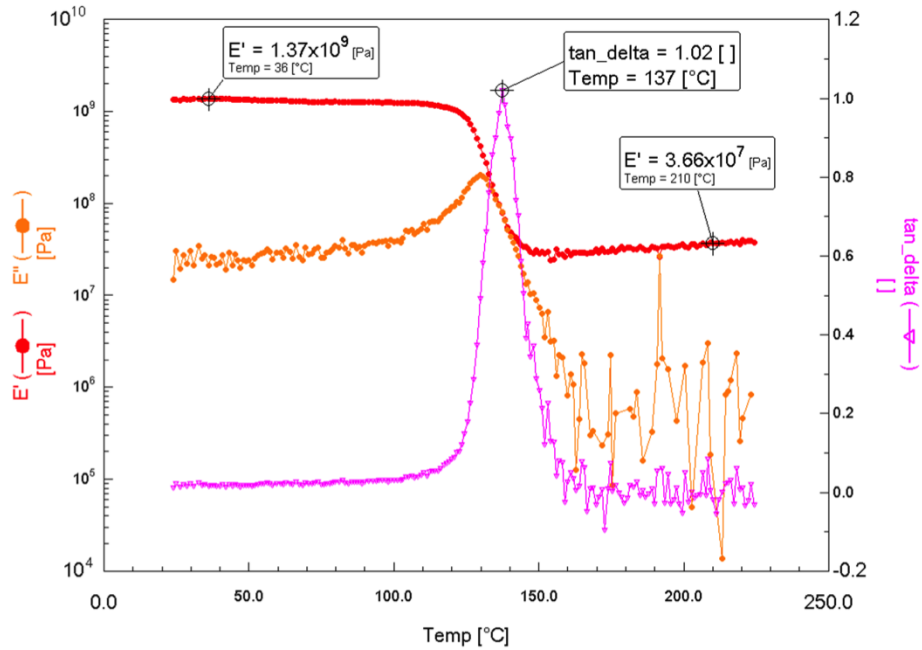
Figure 14. Storage modulus (E'), loss modulus (E'') and tan delta from DMA of lignin-based epoxy resin from DGEBA-IPDA without lignin with 3 point bending mode, with a frequency of 1 Hz, an initial force of 0.5 N and a strain sweep of 0.01%.
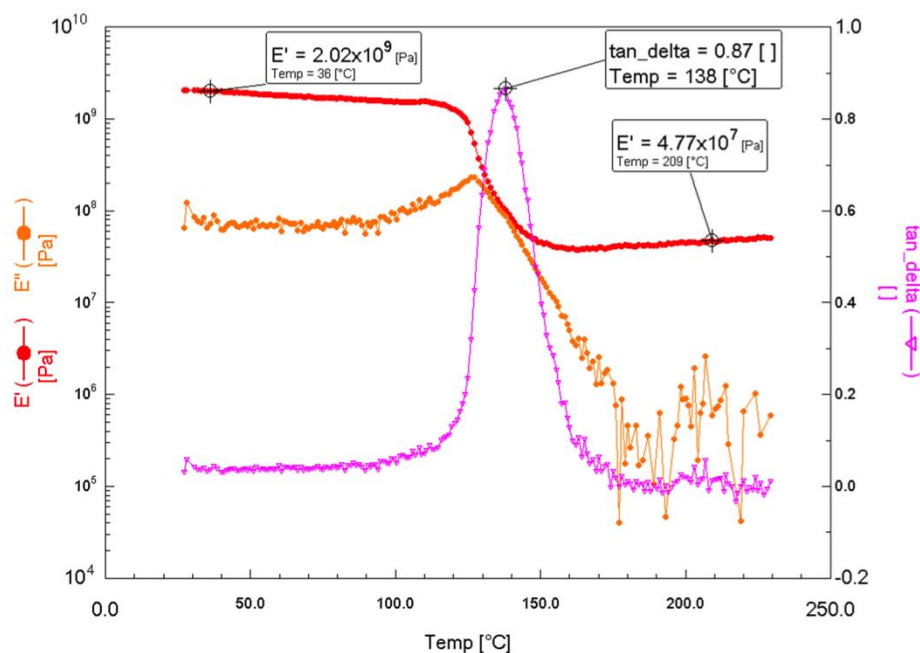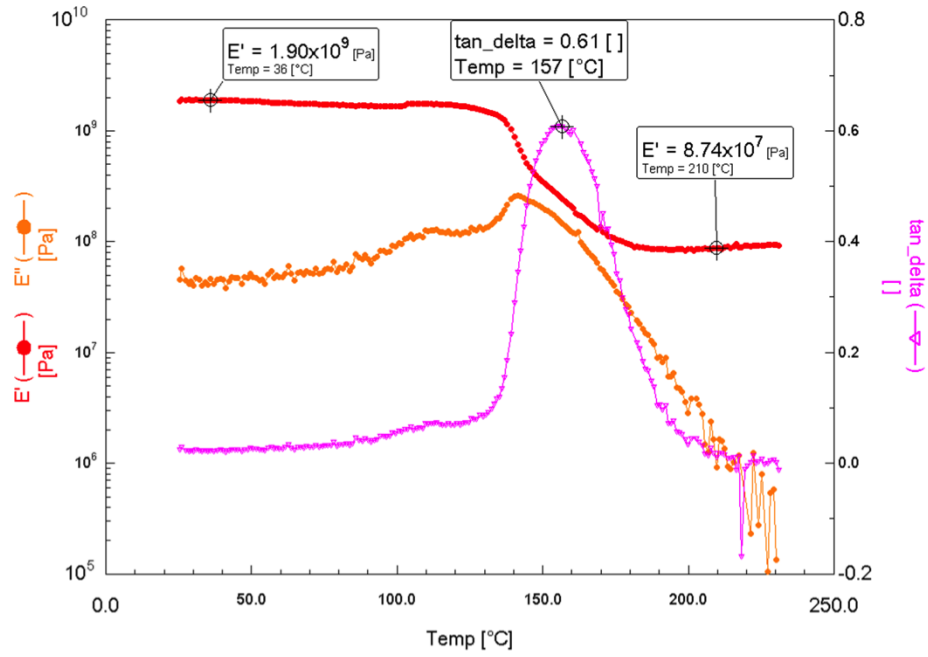
Figure 15. Storage modulus (E'), loss modulus (E'') and tan delta from DMA of lignin-based epoxy resin with 8 wt% lignin with 3 point bending mode, with a frequency of 1 Hz, an initial force of 0.5 N and a strain sweep of 0.01%.
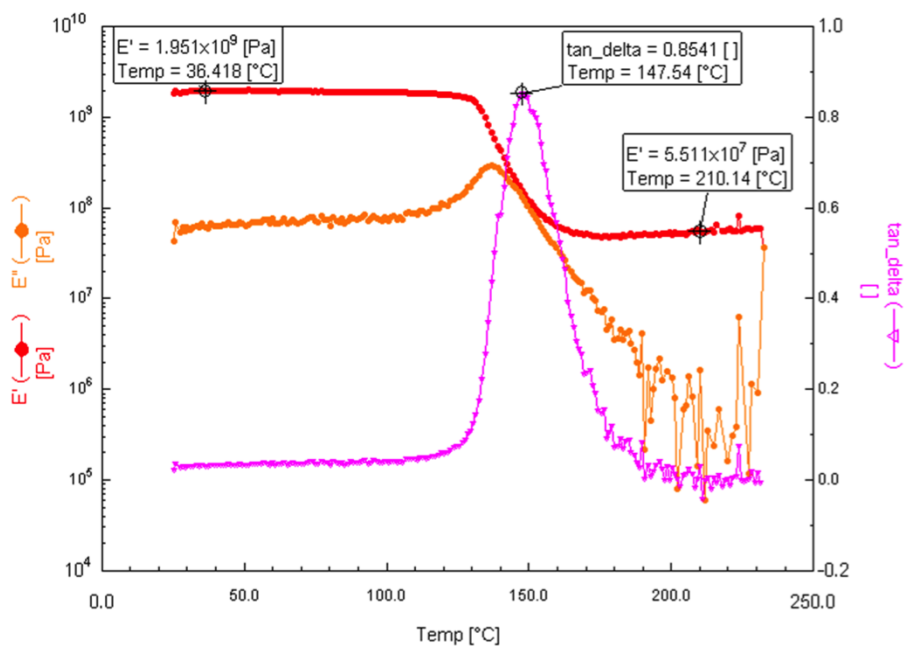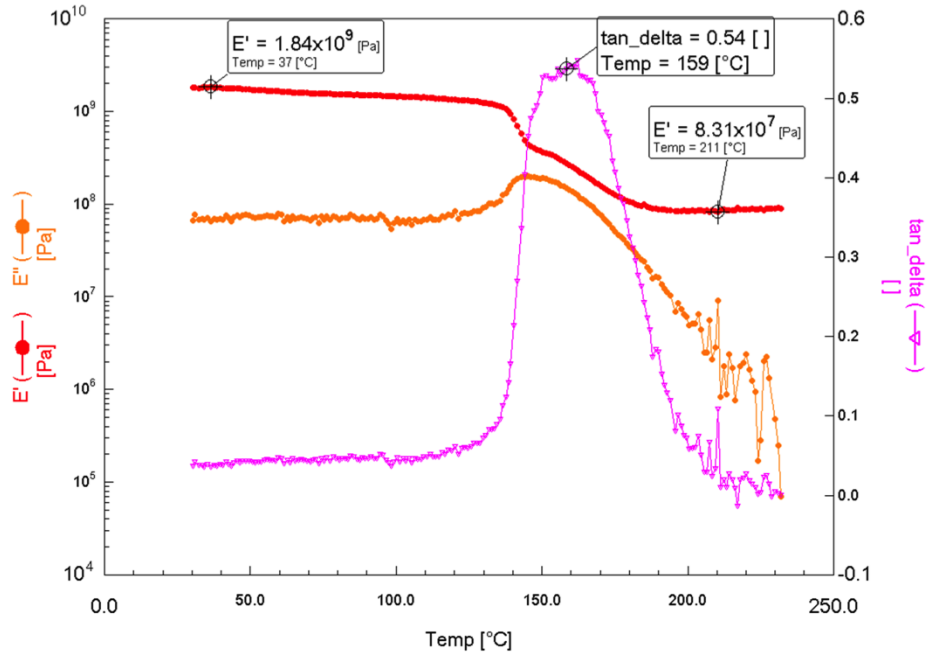

Figure 16. Storage modulus (E'), loss modulus (E'') and tan delta from DMA of lignin-based epoxy resin with 20 wt% lignin with 3 point bending mode, with a frequency of 1 Hz, an initial force of 0.5 N and a strain sweep of 0.01%.
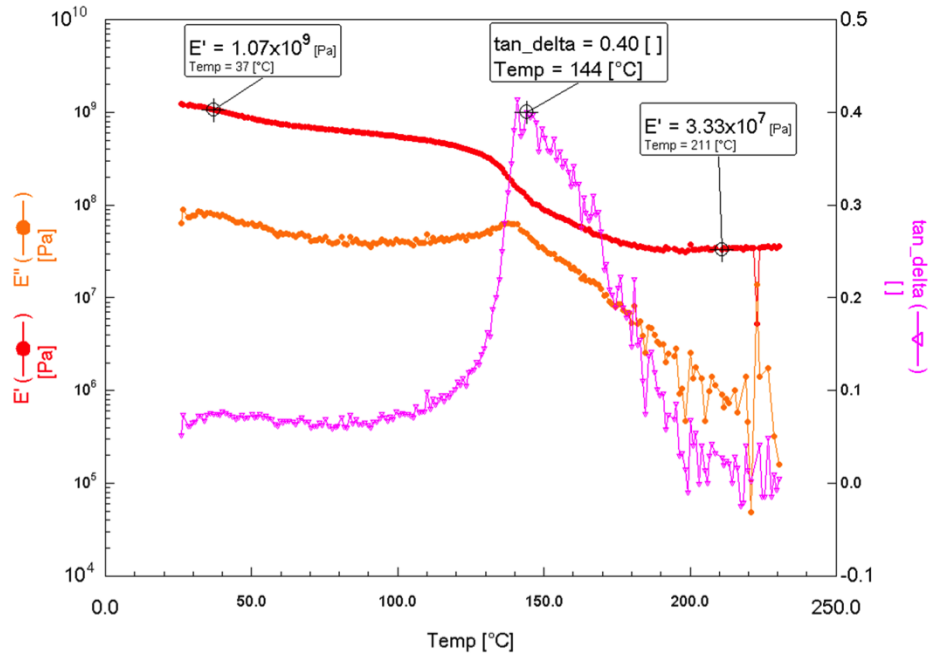
Figure 17. Storage modulus (E'), loss modulus (E'') and tan delta from DMA of lignin-based epoxy resin with 28 wt% lignin with 3 point bending mode, with a frequency of 1 Hz, an initial force of 0.5 N and a strain sweep of 0.01%.

Figure 18. Storage modulus (E'), loss modulus (E'') and tan delta from DMA of lignin-based epoxy resin with 33 wt% lignin with 3 point bending mode, with a frequency of 1 Hz, an initial force of 0.5 N and a strain sweep of 0.01%.

Figure 19. Storage modulus (E'), loss modulus (E'') and tan delta from DMA of lignin-based epoxy resin with 42 wt% lignin with 3 point bending mode, with a frequency of 1 Hz, an initial force of 0.5 N and a strain sweep of 0.01%.
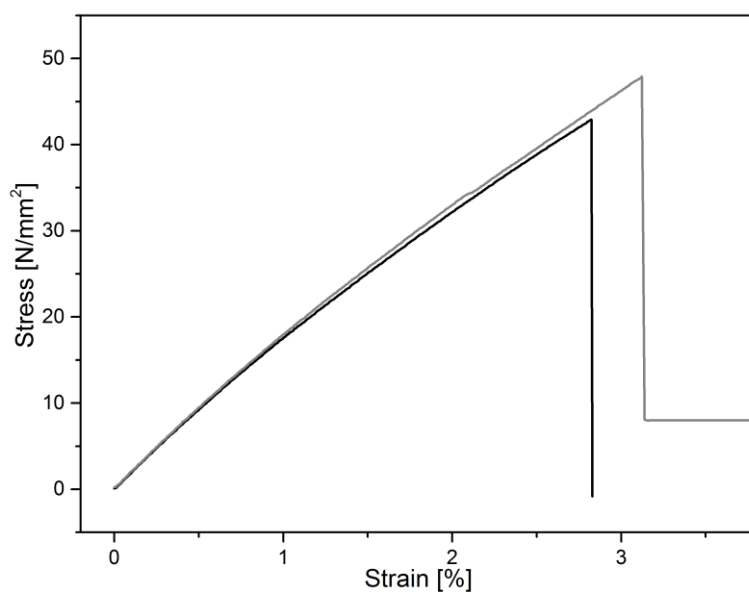
Stress/strain measurements

Figure 20. Stress/strain diagram for DGEBA-IPDA epoxy resin (0 wt% lignin); Conditions: 500 N load cell and a crosshead speed of 1 mm min^{-1}.
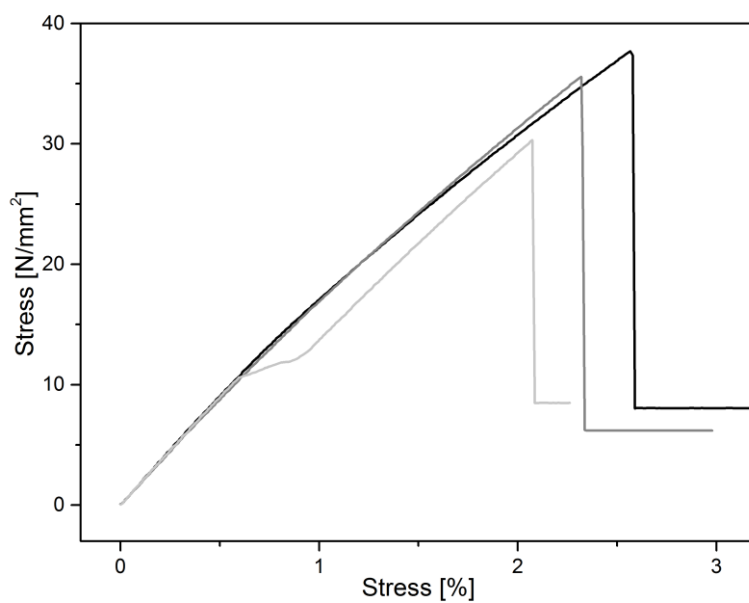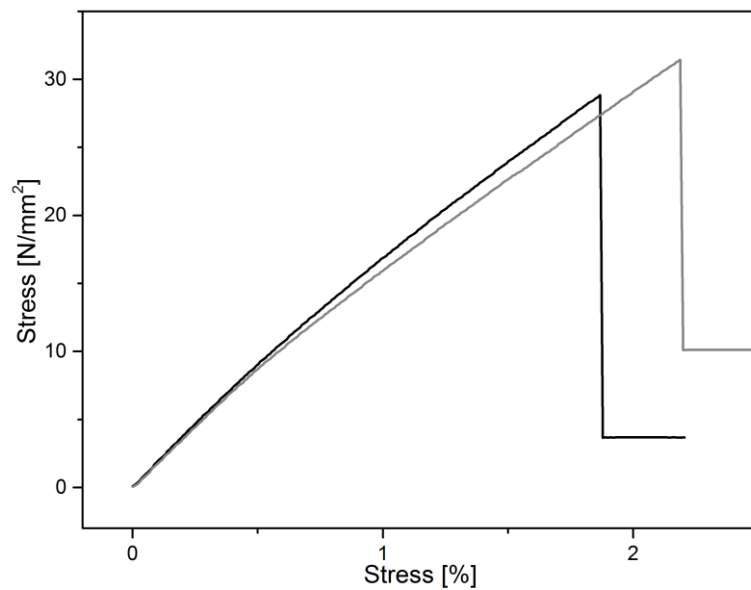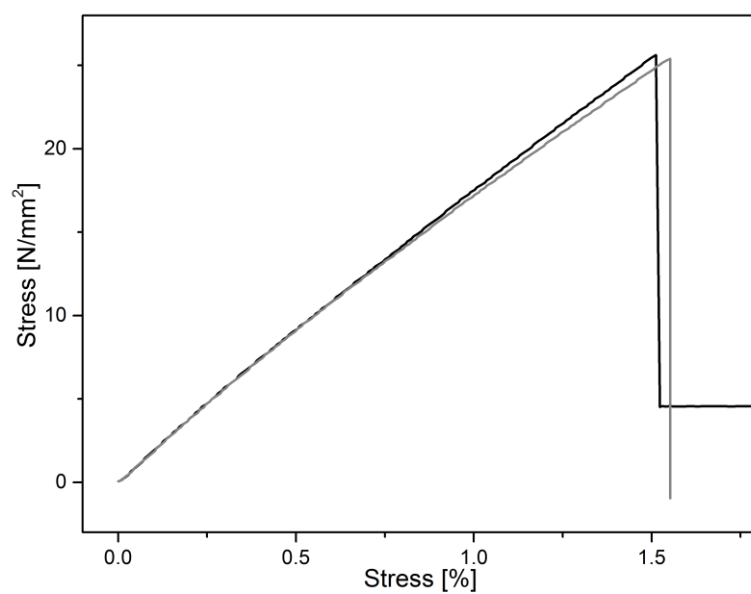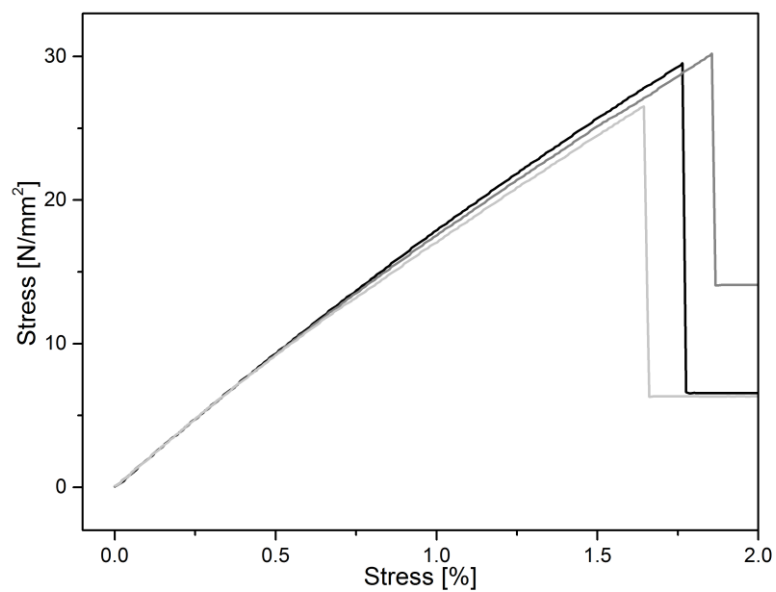

Figure 21. Stress/strain diagram for a epoxy resin with 8 wt% lignin. Conditions: 500 N load cell and a crosshead speed of 1 mm min^{-1}.

Figure 22. Stress/strain diagram for an epoxy resin with 20 wt% lignin; Conditions: 500 N load cell and a crosshead speed of 1 mm min^{-1}.

Figure 23. Stress/strain diagram for an epoxy resin with 28 wt% lignin. Conditions: 500 N load cell and a crosshead speed of 1 mm min^{-1}.

Figure 24. Stress/strain diagram for an epoxy resin with 33 wt% lignin. Conditions: 500 N load cell and a crosshead speed of 1 mm min^{-1}.